To appear in AJ... sometime

Chemical Homogeneity in the Hyades

G.M. De Silva[1], C. Sneden[2], D.B. Paulson[2], M. Asplund[1], J. Bland-Hawthorn[3], M.S. Bessell[1], K.C. Freeman[1]

ABSTRACT

We present an abundance analysis of the heavy elements Zr, Ba, La, Ce, and Nd for Hyades cluster F-K dwarfs based on high resolution, high S/N ratio spectra from Keck/HIRES. The derived abundances show the stellar members to be highly uniform, although some elements show a small residual trend with temperature. The rms scatter for each element for the cluster members is as follows; Zr = 0.055 dex, Ba = 0.049 dex, Ce = 0.025 dex, La = 0.025 dex, Nd = 0.032 dex. This is consistent with the measurement errors, and implies that there is little or no intrinsic scatter among the Hyades members. Several stars thought to be non-members of the cluster based on their kinematics are found to deviate from the cluster mean abundances by about 2σ. Establishing chemical homogeneity in open clusters is the primary requirement for the viability of chemically tagging Galactic disk stars to common formation sites, in order to unravel the dissipative history of early disk formation.

Subject headings: open clusters: individual (Hyades) — stars: abundances

1. INTRODUCTION

One of the major goals of near-field cosmology is to determine the sequence of events involved in the formation of the Galactic disk during the epoch of dissipation. Since the disk formed dissipatively and evolved dynamically, most of the dynamical information is lost.

[1]Mount Stromlo Observatory, Australian National University, Weston ACT 2611, Australia; email: gayandhi@
mso.anu.edu.au

[2]Dept of Astronomy, University of Texas, Austin, TX 78712; chris@verdi.as.utexas.edu

[3]Anglo-Australian Observatory, Eastwood NSW 2122, Australia; jbh@aao.gov.au

However, locked away within the stars, the chemical information survives. If star-forming aggregates have unique *chemical signatures*, we can use the method of chemical tagging to track individual stars back to a common formation site (Freeman & Bland-Hawthorn 2002). With sufficiently detailed abundances we would be able to reconstruct the stellar aggregates which have long since diffused into the Galaxy background. The critical issue for the viability of this method is whether the star-forming aggregates do indeed have unique chemical signatures. The essential first step is to investigate the chemical homogeneity of open clusters which are the likely left overs of star-forming aggregates in the Galactic disk.

Chemical homogeneity in an open cluster implies that the progenitor cloud was uniformly mixed before its stars formed. Theoretical work on star formation in giant molecular clouds suggest the presence of high levels of turbulence (McKee & Tan 2002), which would result in a well mixed gas cloud. However it is not clear whether this mixing occurs during cloud collapse (before the birth of the first stars) or wether few high mass stars form first, shortly after the cloud assembles, and then enrich the cloud uniformly. With both scenarios however, one expects to find homogeneity among the long-lived stars in certain key elements.

The heavier neutron-capture elements are the key to establishing chemical homogeneity, as their abundances are not thought to be modified during normal stellar evolution. The s-process elements are believed to arise from the He burning phase of AGB stars, while the most likely site for r-process elements appears to be type II supernova (Burbidge et al. 1957; Wallerstein et al. 1997). As a result these heavier elements (along with some α and Fe-peak elements), are more representative of the conditions of the progenitor cloud from which the cluster formed. Further, the neutron-capture elements are particularly useful for identifying chemical signatures due to the large intrinsic (cosmic) scatter in their abundances (Edvardsson et al. 1993; Reddy et al. 2003), in particular at low [Fe/H].

Published observations of both light and heavy element abundances in open clusters demonstrate chemical homogeneity, albeit for only a few stars, and lend support to the prospect of chemical tagging. Some recent examples include Friel et al. (2003), who studied the α elements for four giants in the old open cluster Collinder 261 and find 1σ dispersions about the mean, consistent with the expected uncertainties. Schuler et al. (2003) obtained chemical homogeneity for several elements over nine stars in M34, except for K which has a tightly correlated temperature trend, thought to be due to systematic effects in the model atmospheres. Gonzalez & Wallerstein (2000) found homogeneity in Eu for four stars in M11, although there was significant scatter in the α elements. Tautvaišiene et al. (2000) studied 9 stars in M67 and found the heavy element abundances to be almost identical in all stars. Castro et al. (1999) observed that the [Ba/Fe] ratios in the Ursa Major moving group stand out in comparison with solar-neighborhood normal stars with the same metallicity.

We begin our study on chemical homogeneity with the Hyades. It is the nearest cluster to the Sun with age $\approx$ 625Myrs (Perryman et al. 1998) and [Fe/H] $\approx$ 0.13 (Paulson et al. 2003). It has been extensively studied in the past with stellar memberships firmly established (de Bruijne et al. 2001; Hoogerwerf & Aguilar 1999). The Hyades stars have been subject to numerous abundance studies over past years, from Conti et al. (1965) to most recently Paulson et al. (2003) (hereafter Pa03). However to the present date there has been little work done on the abundance analysis of the heavier neutron-capture elements for the Hyades dwarfs. Therefore the present results for heavy element abundances over a large sample of Hyades dwarfs are the first of its kind.

2. CHEMICAL ABUNDANCES

2.1. Observational Data

This study on the neutron-capture elements uses a subset of the data sample analyzed by Pa03. The original observations were part of the planet search program undertaken with the Keck I/HIRES from 1996 to 2000. A full description of the observations can be found in Cochran et al. (2002). Those stars with higher rotation ($v \sin i > 10 \mathrm{km\,s^{-1}}$) were left out of this study due to the poorer spectral resolution and blended lines making it difficult to identify the weak lines of the heavier elements of interest.

The S/N ratio of each spectrum is typically 100 - 200 per pixel and resolving power nominally at 60,000. The spectra cover the wavelength region from 3800Å to 6200 Å, which is an ideal region for the majority of the neutron-capture lines (Bland-Hawthorn & Freeman 2004). Details of the preliminary data reduction procedures can be found in Pa03.

2.2. Model Atmospheres and Spectral Lines

Interpolated Kurucz model atmospheres based on the ATLAS9 code (Castelli et al. 1997) with no convective overshoot were used for this study.

Spectral lines were selected in comparison to the solar atlas (Beckers et al. 1976). Preference was given to clean weaker lines covering a range of excitation potentials. All lines that are formed on or near the wings of other lines were discarded as well as any lines with significant blending. Most of the lines used in this analysis have some degree of blending due to the crowded spectral region where most of the neutron-capture element lines are formed. The full list of lines and references used for this analysis is given in Table 1.

2.3. Abundance Analysis

Details of the stellar parameter analysis are described in Pa03. The same parameters have been used for this study as we are using the same data set.

The abundance analysis makes use of the MOOG code (Sneden 1973) for LTE Equivalent Width (EW) analysis and spectral syntheses. Depending on the degree of blending of the spectral lines, abundances were derived either by EW measurements or by spectral synthesis. The EWs were measured by fitting a Gaussian profile to the observed lines of interest using the interactive *SPLOT* function in the IRAF[1] package. All Zr and Ba abundances were obtained by EW analysis, while the La, Ce, and Nd lines required syntheses. A sample synthesis of Nd lines is shown in Figure 1.

Our analysis produced absolute abundances, but to answer the question of chemical homogeneity in the Hyades, we use differential abundances. The final differential abundances Δ[X/H] were derived by subtracting the absolute abundance of each individual line of the reference star vB153 from the same line in the sample stars, and then taking the mean of the differences for each element. The star vB153 was chosen for reference as it was the reference star used in the differential abundance work by Pa03 hence enabling easy comparisons. By using such a line-by-line differential technique we also reduce the errors due to the uncertainty in the line data, hence minimizing the star-to-star scatter. The differential abundances of all elements are plotted in Figure 2. The absolute abundances for the reference star vB153 is given in Table 2.

2.4. Error Analysis

The main sources of error in the present study are that of EW measurements, continuum placement and stellar parameters. External errors, such as uncertainties in the line data and model atmospheres are the least sources of error since we are interested only in the differential abundances. The number of lines used to calculate the final abundances also contributed to the total uncertainty for each element.

The error in EWs estimated by repeated measurements of each line, is between 0.5mÅ to 5mÅ depending on the strength of the lines, corresponding to abundance errors of 0.01 dex to

[1]IRAF is distributed by the National Optical Astronomy Observatory, which is operated by the Association of Universities for Research in Astronomy, Inc., under cooperative agreement with the National Science Foundation.

0.05 dex. The measurement errors for the synthesised abundances were derived by changing the abundance until there is a clear visible deviation from the best fit. The differential error in the stellar parameters were assumed to be $\delta T_{eff} = 50$K, $\delta \log\, g = 0.1$ cm s^{-2} and $\delta\xi = 0.1$ km s^{-1}. Table 3 shows the abundance dependence on the stellar parameters. Typical values of the total estimated uncertainty in each element is as follows; Zr = 0.048 dex, Ba = 0.047 dex, La = 0.025 dex, Ce = 0.025 dex, and Nd = 0.026 dex.

3. ABUNDANCE TRENDS

The final results show uniform abundances although some elements show a small residual trend with temperature. Slightly increasing slopes are seen for Zr, while decreasing trends are seen for La and Nd. It is very likely that these trends are a systematic effect resulting from inadequecies in the model atmospheres, and does not reflect intrinsic abundance variations of the Hyades cluster.

3.1. Stellar Parameters

The abundances for the α and Fe-peak elements by Pa03 show no trends such as seen here for the neutron-capture elements (except for Ca which has an increasing slope with temperature thought to be due to saturating Ca lines in the cooler stars). Since we have used the same stellar parameters, it is unlikely that errors in the parameters caused the presently observed trends. Furthermore, any change in the model parameters will not correct all the trends as different elements show trends in opposite directions. As a check, each parameter (T_{eff}, log g, and micro-turbulence) was varied in an attempt to remove the trends. For effective temperature, the coolest stars were made cooler and hottest stars made hotter by $\delta T_{eff} = 100$K. Similarly the surface gravity was varied by $\delta \log\, g = 0.1$ cm s^{-2} and micro-turbulence by $\delta\xi = 0.1$ km s^{-1}. Such a change will *flatten* the slopes for La and Nd, while the same changes increase the slopes of Ba and Zr abundances.

Also to further confirm of our method of analysis, we re-analyzed the Mg abundances for a sub-sample of stars covering the full temperature range, and successfully recovered the results of Pa03, which does not show any trends. A comparison plot is shown in Figure 3. The mean of the difference Δ[Mg/H]$_{\rm this\ study}$ - Δ[Mg/H]$_{\rm Pa03}$ = 0.02 dex, with a standard deviation of 0.03 dex.

3.2. Continuum Placement

Note that the scatter for all elements increase with lower temperature. As the temperature decreases, the greater the blending and therefore the harder it is for continuum placement. Since most lines lie in the blue part of the spectral region which is highly crowded, determining the continuum level was difficult. It is possible that as the lines begin to blend in the cooler stars, the continuum is placed too low and a lower abundance is estimated for the cooler stars in comparison to the stars at the hotter end. Such an effect would explain the increasing trends observed for Zr, but we cannot explain the decreasing slopes as due to an error in continuum placement.

3.3. Hyperfine Structure

Many of the heavy element lines are affected by hyperfine structure. In most cases the effects are small enough to be negligible, especially in very weak lines. However as lines saturate and move off the linear part of the curve of growth, these effects become more important. If an observed line is made up of many components, which are greater than the intrinsic width of the line as calculated by standard means of broadening (thermal, micro-turbulence, etc.) then neglecting the splitting would result in over estimating the abundance value. The transition lines for La, which has widely known hyperfine structure have been synthesised accordingly. However a slight slope is still present in the La results after accounting for the hyperfine structure.

3.4. NLTE Effects

Finally we suspect that NLTE effects may play a role in these abundance trends. NLTE effects are specific to the atom and affect each element differently rather than generally (cf. stellar parameters). Since we observe slopes in opposite directions, it is very likely that we are seeing NLTE effects. Unfortunately there have not been many NLTE calculations done for the heavier neutron-capture elements in order to determine what the such effects would be. Mashonkina et al. (1999) find that for the BaII line at 5853Å the correction is less than 0.1 dex, however it does not cover the full range of temperatures we are covering in this analysis. We are more interested to see if NLTE effects come into play over a large range of temperatures in order to explain the observed abundance trends. We are not aware of any published work that indicate such NLTE effects.

A study of NLTE effects for heavy elements is beyond the scope of this paper, but in

an attempt to quantify this possible NLTE correction we have fitted least square regression lines to the observed trends. The fits are in the form of Δ[X/H] = $\alpha + \beta(5200\mathrm{K}/T_{eff})$ where T_{eff} has been normalised by the T_{eff} of the reference star vB153. The values of α and β are given for each element in Table 4. We look forward to future NLTE calculations which may explain the presently observed abundance trends.

4. DISCUSSION

4.1. Chemical Homogeneity

With regards to chemical homogeneity and establishing chemical signatures for the Hyades, our results are positive. The tightly correlated abundances are an indication of the level of homogeneity that exists within the cluster. The observed scatter for the Hyades members σ_{obs}, estimates of the intrinsic scatter σ_{int}, and the corresponding Chi squared value, is given in Table 5. σ_{int} was estimated using the equation, $\sigma^2_{obs} = \sigma^2_{int} + \sigma^2_{expected}$, and $\chi^2_r = \sigma^2_{obs}/\sigma^2_{expected}$, where $\sigma_{expected}$ is the estimated uncertainty as discussed in Section 2.4. With the estimated uncertainties being typically around σ_{obs}, then $< \chi^2_r > \approx 1$. This implies that the total star-to-star scatter is within the measurable limit and that the true intrinsic scatter among the Hyades stellar members are extremely low.

This level of chemical uniformity is observational evidence for a chemically well mixed gas cloud. It is possible that these dwarfs formed later after the high mass stars have evolved to produce several supernova, which enriched the gas as well as contributed to the mixing of the gas cloud. Although the actual mechanism for the mixing is still debatable, it is clear from our results that the gas cloud was uniformly mixed by the time these dwarf stars formed.

Also, the detected levels of chemical homogeneity indicates that these stars have not been *polluted* either from local sources (such as stellar winds, supernova explosions), or from swept up gas from the ISM. Quillen (2002) derived an upper limit of 0.03 dex for the star-to-star metallicity scatter using the Hyades H-R diagram, indicating that pollution effects are not common and strong. Our estimated σ_{int} for the heavier elements is within this upper limit.

4.2. Stellar Membership

Further reasons to interpret the results as a strong case for homogeneity and positive signs of establishing a chemical signature is the deviation of a few stars that are thought to be non-members found in the same direction of the cluster. The two stars vB1 and vB2 are clearly over abundant by over 2σ in all elements. Pa03 also found these stars to be significantly enriched. These stars were earlier considered as Hyades members as they have consistent photometry, radial velocities, and Hipparcos distances for membership, however de Bruijne et al. (2001) find that they are non-members based on proper motions and trigonometric parallax measurements. The star HD14127 is under abundant in Zr, Ce, La, and Nd, however it is slightly over abundant in Ba. Pa03 classes it as a non-member due to its metallicity being -0.25 dex below the cluster mean, its Hipparcos distance being too large, and it lies below the Hyades main sequence.

4.3. Implications for Chemical Tagging

Since most of the dynamical information of the Galactic disk has been subject to evolutionary processes of dissipation and scattering, chemical information locked within the stars provide the only true tracer left of initial identity. Having established the Hyades open cluster members to be homogeneous in the heavier neutron-capture elements along with the α and Fe-peak elements (Pa03), and the fact that several non-members deviate from the cluster mean, supports the case for using chemical abundances as tracers of cluster membership and establishing chemical signatures unique only to the stellar members of the cluster. We are more confident now that chemical information can be used to identify the larger star-forming aggregates in the early disk by means of chemical tagging.

This paves the way for chemically tagging other member stars which are at present no longer part of the bound Hyades cluster system. A necessary test would be to study the stars of the Hyades super-cluster, which is thought to be a moving stellar group (cf. Eggen 1970). It will be very interesting indeed to check if the same abundance patterns are seen among the stellar members of the super-cluster as in the core of the Hyades open cluster we have presented here. Such a test will be the next step forward in truly demonstrating the viability of chemical tagging for the future.

This research has made use of the Vienna Atomic Line Database (VALD), operated at Vienna, Austria, and the Database on Rare Earths At Mons University (D.R.E.A.M.), operated at Mons, Belgium.

REFERENCES

Beckers, J. M., Bridges, C. A., & Gilliam, L. B. 1976, A high resolution spectral atlas of the solar irradiance from 380 to 700 nanometers. Volume 2: Graphical form

Bland-Hawthorn, J., & Freeman, K. C. 2004, Publications of the Astronomical Society of Australia, 21, 110

Burbidge, E. M., Burbidge, G. R., Fowler, W. A., & Hoyle, F. 1957, Reviews of Modern Physics, 29, 547

Castelli, F., Gratton, R. G., & Kurucz, R. L. 1997, A&A, 318, 841

Castro, S., Porto de Mello, G. F., & da Silva, L. 1999, MNRAS, 305, 693

Cochran, W. D., Hatzes, A. P., & Paulson, D. B. 2002, AJ, 124, 565

Conti, P. S., Wallerstein, G., & Wing, R. F. 1965, ApJ, 142, 999

de Bruijne, J. H. J., Hoogerwerf, R., & de Zeeuw, P. T. 2001, A&A, 367, 111

Den Hartog, E. A., Lawler, J. E., Sneden, C., & Cowan, J. J. 2003, ApJS, 148, 543

Edvardsson, B., Andersen, J., Gustafsson, B., Lambert, D. L., Nissen, P. E., & Tomkin, J. 1993, A&A, 275, 101

Eggen, O. J. 1970, PASP, 82, 99

Freeman, K., & Bland-Hawthorn, J. 2002, ARA&A, 40, 487

Friel, E. D., Jacobson, H. R., Barrett, E., Fullton, L., Balachandran, S. C., & Pilachowski, C. A. 2003, AJ, 126, 2372

Gonzalez, G., & Wallerstein, G. 2000, PASP, 112, 1081

Hoogerwerf, R., & Aguilar, L. A. 1999, MNRAS, 306, 394

Kupka, F., Piskunov, N. E., Ryabchikova, T. A., Stempels, H. C., & Weiss, W. W. 1999, A&AS, 138, 119

Lawler, J. E., Bonvallet, G., & Sneden, C. 2001, ApJ, 556, 452

Mashonkina, L., Gehren, T., & Bikmaev, I. 1999, A&A, 343, 519

McKee, C. F., & Tan, J. C. 2002, Nature, 416, 59

Paulson, D. B., Sneden, C., & Cochran, W. D. 2003, AJ, 125, 3185

Perryman, M. A. C., Brown, A. G. A., Lebreton, Y., Gomez, A., Turon, C., de Strobel, G. C., Mermilliod, J. C., Robichon, N., Kovalevsky, J., & Crifo, F. 1998, A&A, 331, 81

Piskunov, N. E., Kupka, F., Ryabchikova, T. A., Weiss, W. W., & Jeffery, C. S. 1995, A&AS, 112, 525

Quillen, A. C. 2002, AJ, 124, 400

Reddy, B. E., Tomkin, J., Lambert, D. L., & Allende Prieto, C. 2003, MNRAS, 340, 304

Ryabchikova, T. A., Piskunov, N. E., Stempels, H. C., Kupka, F., & Weiss, W. W. 1999, Physica Scripta, 162

Schuler, S. C., King, J. R., Fischer, D. A., Soderblom, D. R., & Jones, B. F. 2003, AJ, 125, 2085

Sneden, C. A. 1973, Ph.D. Thesis

Tautvaišiene, G., Edvardsson, B., Tuominen, I., & Ilyin, I. 2000, A&A, 360, 499

Wallerstein, G., Iben, I. J., Parker, P., Boesgaard, A. M., Hale, G. M., Champagne, A. E., Barnes, C. A., Käppeler, F., Smith, V. V., Hoffman, R. D., Timmes, F. X., Sneden, C., Boyd, R. N., Meyer, B. S., & Lambert, D. L. 1997, Reviews of Modern Physics, 69, 995

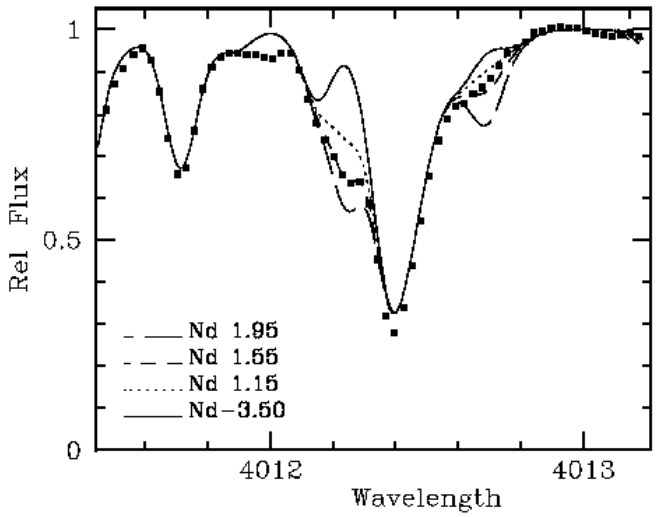

Fig. 1.— Sample synthetic (dashed and dotted curves) and observed (dots) spectra of the two NdII lines at 4012.24 Å and 4012.69 Å.

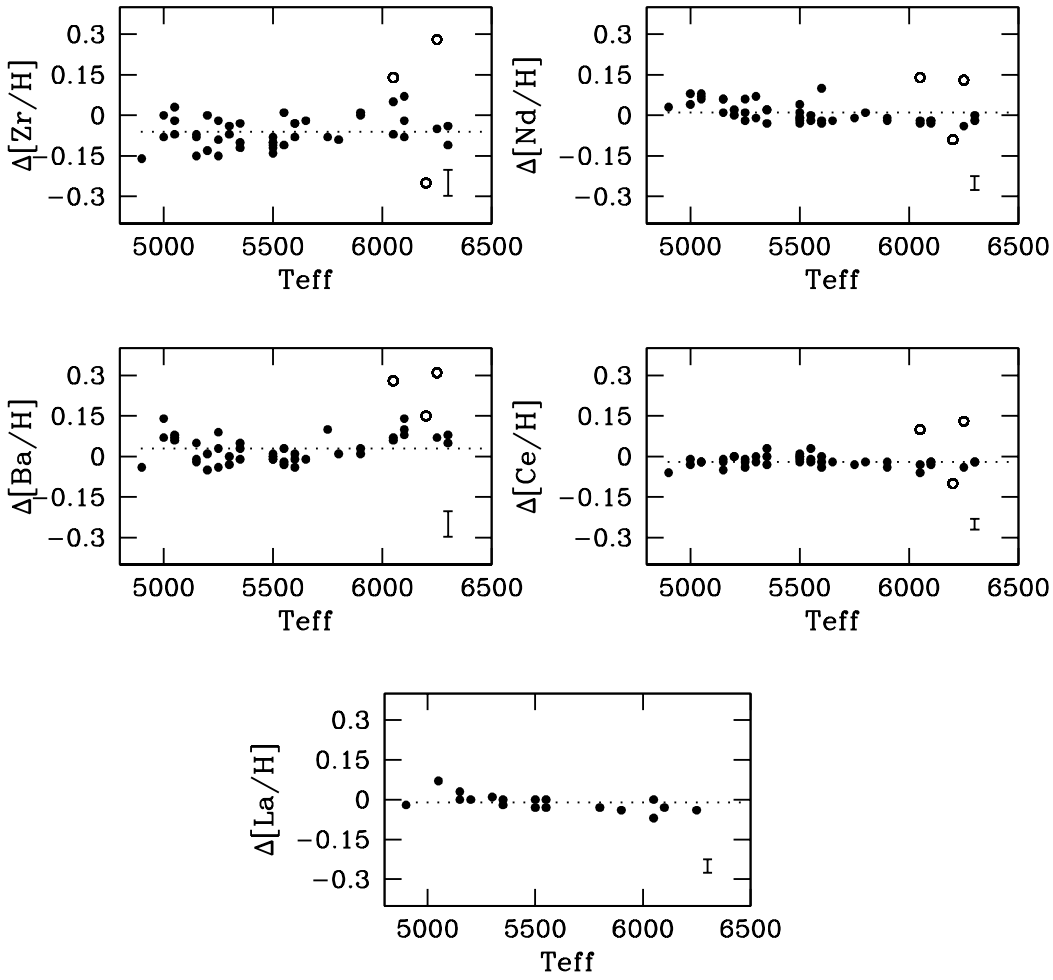

Fig. 2.— Differential [X/H] vs. effective temperature. The differential comparision star is vB153 as discussed in the text. The open symbols are stars believed to be non-members as discussed in Section 4.2. The dashed lines are mean abundance levels. The error bars shown is the typical abundance uncertainty for each element.

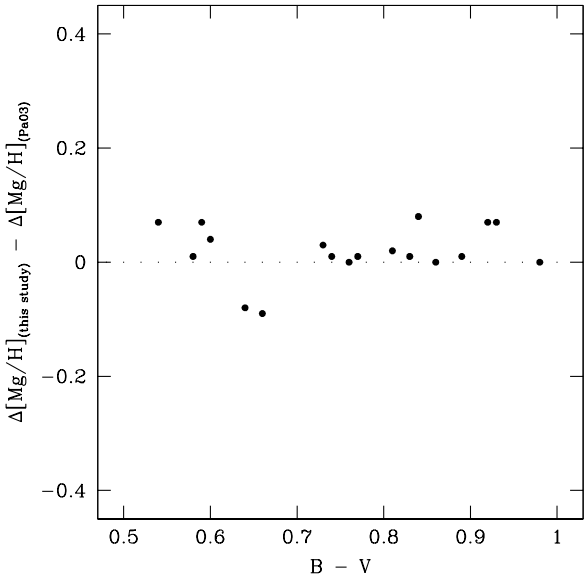

Fig. 3.— Comparison of Mg abundances with Pa03 for a sub-sample of stars covering the full temperature range. The mean of the difference Δ[Mg/H]$_{\rm this\ study}$ - Δ[Mg/H]$_{\rm Pa03}$ is 0.02 dex, with a standard deviation of 0.03 dex, but most importantly no slope is present.

Table 1. Line List

Element	Wavelength	χ (eV)	log gf	Ref
ZrII	4050.33	0.710	-1.000	1
BaII	4130.57	2.722	0.680	1
BaII	4554.04	0.000	0.170	1
BaII	4934.09	0.000	-0.150	1
BaII	5853.69	0.604	-1.000	1
BaII	6141.73	0.704	-0.076	1
LaII	3988.52	0.400	0.210	2
LaII	3995.75	0.170	-0.060	2
LaII	4086.71	0.000	-0.070	2
LaII	4662.50	0.173	-1.240	2
CeII	4083.22	0.701	0.270	3
CeII	4364.65	0.495	-0.230	3
CeII	4562.36	0.478	0.230	3
CeII	4628.16	0.516	0.200	3
NdII	4012.24	0.630	0.810	4
NdII	4012.69	0.000	-0.600	4
NdII	4018.82	0.063	-0.850	4
NdII	4068.89	0.000	-1.420	4
NdII	4462.98	0.559	0.040	4

References. — (1) From Vienna Atomic Line Database (VALD) (Kupka et al. 1999; Ryabchikova et al. 1999; Piskunov et al. 1995). (2) Lawler et al. 2001 (3) Palmeri et al. 2001 (http://www.umh.ac.be/astro/dream.shtml) (4) Den Hartog et al. 2003

Table 2. Elemental Abundances for vB153

	[Zr/H]	[Ba/H]	[La/H]	[Ce/H]	[Nd/H]
vB 153	2.73	2.60	1.19	1.77	1.45

Table 3. Abundance Dependencies on Model Parameters

Star ID	Model Parameter	δ[Zr/H]	δ[Ba/H]	δ[La/H]	δ[Ce/H]	δ[Nd/H]
vB 25	$T_{\rm eff}\pm50$	±0.01	±0.02	±0.01	±0.01	±0.02
($T_{\rm eff}$ = 4900)	log $g\pm0.1$	±0.03	0.00	±0.01	0.00	0.00
	$\xi\pm0.1$	∓0.02	∓0.03	±0.02	0.00	±0.02
vB 105	$T_{\rm eff}\pm50$	±0.01	±0.02	±0.01	±0.01	0.00
($T_{\rm eff}$ = 6100)	log $g\pm0.1$	±0.04	±0.01	0.00	±0.01	±0.02
	$\xi\pm0.1$	∓0.02	∓0.03	±0.01	0.00	0.00

Table 4. Regression Line Parameters

Element	α	β
Zr II	2.88	-0.22
Ba II	2.81	-0.19
La II	0.90	0.29
Ce II	1.72	0.04
Nd II	1.11	0.37

Table 5. Abundance Scatter

Element	σ_{obs}	σ_{int}	χ^2_r
Zr	0.055	0.026	1.30
Ba	0.049	0.013	1.08
La	0.025	0.000	1.00
Ce	0.025	0.000	1.00
Nd	0.032	0.018	1.51